Development of a Simple Device for Field Air Flow Measurement of Residential Air Handling Equipment

Final Report

Larry Palmiter
Paul W. Francisco

Ecotope, Inc.
2812 E. Madison St.
Seattle, WA 98112

March, 1998

Prepared for the U. S. Department of Energy under Small Business Technology Transfer Grant #DE-FG03-97ER86060

DOE Project Officer: Esher R. Kweller

Introduction

This project is a direct response to the Small Business Technology Transfer (STTR) solicitation, from which we quote:

"The proper flow of conditioned air through duct distribution systems is required for proper operation within an installation. Manufacturers design heating and cooling equipment for a specified amount of air flow over a coil or heat exchanger. Unfortunately, there is no easy way for an installer to quantify this air flow when the unit is installed. In order to provide an accurate measurement, current portable air flow measuring devices require more care in their proper use to obtain an accurate result than installers have time to provide. Grant applications are sought for air flow measurement devices and techniques that are easy to use and give repeatable, accurate results."

The primary emphasis in the solicitation is on verification that air flow is within the range specified for a particular piece of equipment. This is especially important for avoiding low flow in heat pumps and air conditioners, as this can lead to significant performance penalties. For this purpose, an accuracy of plus or minus 10 percent is more than adequate.

Another application for such a flow measurement device is the estimation of duct efficiency. The flow through the air handler is a key parameter in the efficiency equations. For this purpose, it is desirable to have the most accuracy possible. After some discussion among project team members, it was decided to aim for a goal of plus or minus 5 percent accuracy over a range of flows from about 60 to 100 percent of the rated capacity, and a variety of possible return plenum configurations.

Phase I of the STTR grant is a proof-of-concept study of the proposed measurement device. Additional development and refinement is relegated to Phase II.

This report details the development and evaluation of a promising device based upon a perforated plate which can be inserted into a filter slot in place of the filter. In use, a single 30-second average pressure difference is measured with a handheld digital micro-manometer. To obtain the flow, the pressure difference is entered into a simple discharge coefficient equation.

The project team consisted of three agencies: Ecotope, Inc., the small business concern receiving the grant; Washington State University (WSU), the research institution; and The Energy Conservatory (TEC), another small business and the potential manufacturer of the device. The team members included Larry Palmiter (Principal Investigator) and Paul Francisco of Ecotope; Gary Nelson, Ron Rothman, and Collin Olson of TEC; and Johnny Douglas and Michael Lubliner of WSU.

The test facility was the HVAC Technician Training shop at Clover Park Technical College in Tacoma, WA. They were able to provide floor space and a selection of air handlers for test purposes. We would like to acknowledge the cooperation of Clover Park faculty members Carl Byrd and Don Pearce without whose assistance this work would not have been possible. The

trade school ambiance lent a certain real-world atmosphere to the testing. One corner of the test facility with team members at work is shown in Fig. 1.

The authors gratefully acknowledge the special contributions of the other team members. Collin Olson of TEC created the custom data logging software used for all of our measurements; Johnny Douglas of WSU assisted with all of the test runs and created the drawings of the test setups; Ron Rothman of TEC designed and built the final flow plate prototype; Michael Lubliner of WSU provided the photographs used in this report; and Gary Nelson of TEC contributed many useful suggestions concerning all aspects of the project.

Fig. 1 The test facility and several team members. From left to right: Ron Rothman, Gary Nelson, Paul Francisco, Johnny Douglas, and Larry Palmiter.

Evolution of the Prototype

Exploratory Tests

The initial concept, due to Larry Palmiter of Ecotope, was to use a plain perforated plate in the air handler filter slot. The upstream to downstream pressure difference measured with a digital time-averaging micro-manometer would be entered into a calibration formula to obtain the flow.

Exploratory tests were performed at Ecotope using two plain 20x20 inch perforated plates masked with duct tape along the edges to provide an 18x18 inch square net opening. This matches a standard 20x20 filter and guarantees that the unmasked area of the plate was determined by design and not by the protruding lips of the filter slot. One plate had $^{3}/_{32}$-inch diameter holes and a free area of 32% and the second one had ¼-inch diameter holes and a free area of 40%. The plates were mounted on one end of a cardboard box and discharged directly

into the atmosphere. Pressures were measured with pitot tubes at each of the four corners upstream of the plate and referenced to the atmosphere. A 10- or 14-inch diameter round duct entered either the top or side of the box, so as to simulate either straight-through flow or flow making a right angle. The flow was provided and measured by a Duct Blaster® at the upstream end of the duct. The average of the four pressures and the flow were used to calculate a generalized discharge coefficient as the flow in cubic feet per minute (cfm) divided by the square root of the average pressure in Pascals (Pa). These tests resulted in three important observations:

The discharge coefficients were highly sensitive to whether the duct had a top entry or a side entry.

The discharge coefficients were highly sensitive to the diameter of the duct.

The plate with 32% free area was less sensitive than the one with 40% free area.

These observations led us to configure the test setup to verify the same effects when using an actual air handler and to design a set of return plenum arrangements to vary the diameter and type return duct entry.

Preliminary Testing

At the test facility an electric furnace air handler with a nominal rating of 855 cfm at an external static pressure of 75 Pa was selected for all of the subsequent tests in the prototype development and evaluation. This unit had a filter slot 20 inches square. A return plenum 20x20 in. and 24 inches tall was fabricated for the air handler. Two 14-inch diameter round collars were attached to the plenum, one centered in the top of the plenum and the other one centered in one side of the plenum. In use, one of the collars was sealed; the other was used for the return flow.

Filter pressure drops are generally given for design face velocities of 300 feet per minute (fpm). Recommended return duct velocities are around 700 fpm, corresponding to an expansion ratio of 2.3. The transition from 14 inch round to the perforated plate gave an expansion ratio of about 2.1, and at a flow of 800 cfm the average velocity in the 14-inch duct was 748 fpm and the face velocity at the plate was 356 fpm.

The 32% free area plate was installed in the air handler at the test facility. The first attempts were done using one Duct Blaster® upstream of the plate. Because this resulted in the measurement device “pushing” the air into the system the flow pressure data were very noisy. The Duct Blaster® was then moved to the downstream end of the furnace and pulled air through the system. However, this configuration requires a TEC flow conditioner and a ring for accurate results and the resulting extra pressure drop prevented attainment of the higher flow values.

The solution to this problem was to use two Duct Blasters®, one upstream and one downstream of the furnace. The upstream Duct Blaster® was not powered and was used solely as a measurement device. The downstream Duct Blaster® was attached by a 10 ft flexible duct to the supply side of the air handler. No measurements were made with the downstream Duct

Blaster®. This combination of devices allowed the flow to be smoothly varied from 250 cfm to 850 cfm. For low flows, the downstream Duct Blaster® was used alone to pull air through the entire system including the air handler blower. For higher flows, the air handler blower was turned on and the downstream fan provided a variable boost. In this configuration air is pulled instead of pushed through the upstream Duct Blaster® which resulted in accurate measurements of the flow.

The upstream measurement device terminated in a 10-inch round fitting which was fitted to a short 10-inch to 14-inch expander. The expander was fitted either directly to one of the 14-inch collars on the return plenum, to a standard short radius 14-inch round elbow which was then connected to the collar, or to a 10-foot section of 14-inch round duct which was then connected to the collar. The 10-foot duct provided a fairly well developed flow at the collar and a 14-inch round jet entering the return plenum. The direct connection without the duct resulted in a 10-inch round jet about 6 inches upstream of the plenum. This configuration represents a worst case situation with a high expansion ratio. Figure 2 shows the test setup in the top entrance, no-duct configuration. Figure 3 shows the test setup in the side entrance configuration with the 10-foot duct. As shown in both Figs. 2 and 3, the entire system was mounted horizontally on the floor of the facility.

Fig. 2. Test setup in top, no duct or elbow

Fig. 3. Test setup in side with 10’ duct

The ducts, fittings and return plenum were well sealed with duct tape and masking tape for all components between the perforated plate and the flow measurement device. Leakage in this section of the system affects the absolute calibration factors because the flow through the perforated plate is greater than the flow through the measurement device. One test of the leakage was made by replacing the perforated plate with a piece of cardboard sealed in place and pressurizing the return system with a Duct Blaster®. The leakage measured with Ring 3 of the Duct Blaster® was 18 cfm at 50 Pa pressurization. When additional detailed inspection and sealing of tiny holes around pitot tube and sensor penetrations and joints in the plenum were made, the leakage dropped to 15 cfm at 50 Pa, a reduction of 17 percent. The negative pressure in the return plenum in the normal test mode at 800 cfm was about 90 Pa. The leakage under these conditions, assuming an flow exponent of 0.5 and 18 cfm at 50 Pa, would be about 25 cfm or 3.2 percent of the flow. Naturally, there are variations in the degree of sealing from one set of runs to the next, since ducts and fitting are taken apart and reconnected and sealed. Based on the

drop from 18 to 15 cfm, these variations could be 20 to 40 percent of the leakage. This would produce variations of about 0.6 to 1.2 percent of the flow under calibration conditions.

The first set of pressure drop measurements across the plate were made at each of the four corners both upstream and downstream of the perforated plate. The corners were considered the most preferable measurement location from the perspective of commercial ease of manufacture of the device. Flows were measured at seven flow stations from 550-850 cfm in 50 cfm increments. The difference between the upstream average pressure and the downstream average pressure for each measurement point was used to calculate a discharge coefficient assuming a square-root relationship between flow and pressure drop. A number of calibration runs were done with various return duct system configurations.

The worst case results occurred with no duct between the upstream Duct Blaster® and the plenum. The average discharge coefficients are shown in the first line of Table 1. There was about a 32% difference in the calibration for the side entrance versus the top entrance. Examination of the four individual corner pressure differences showed as much as a 30% difference between the highest and lowest values.

These results were considered unacceptable. It was clearly necessary to measure pressures that better represented the flow velocity. In order to accomplish this, the net area of the perforated plate was divided into four equal quadrants. In the center of each quadrant pitot tubes were mounted facing into the flow both upstream and downstream of the plate. The static taps of the pitot tubes were used for measuring pressures. This arrangement produced a large improvement in the calibration results, with the side entrance within 13% of the top entrance. These results are shown in line 2 of Table 1.

Although this was a significant improvement, the quadrant taps with pitot tubes was not an arrangement that could fit through the filter slot and would also be delicate and expensive to manufacture. It was also clear that more pressure measurement points would be required, and that one of the problems was that the jet from the top entrance did not fully expand and tended to blow through the center of the plate. These results were communicated to Ron Rothman, the design engineer at TEC, who has much practical experience with flow measurement and was responsible for the design of the final prototype. As shown in the final row of Table 1, the variation for side versus top entry without the duct for the resulting prototype, which is discussed in the next section, was reduced to 0.9%. This result was considered highly satisfactory, especially considering that this was only the proof-of-concept phase of the project.

Table 1. Impact of Geometry and Pressure Tap Arrangement on Discharge Coefficient, cfm/Pa$^{0.5}$

	Top	Side	Percent difference
Corner taps	178.4	121.5	31.9
Quadrant taps	189.7	165.9	12.5
Prototype	139.3	138.0	0.9

Final Prototype and Testing

The prototype used the plate with 40% free area because the design required that the central portion of the plate be obstructed to counteract jet effects. The prototype is shown in Figs. 4 and 5. Note that the photograph in Fig. 4 was taken with the original prototype which had a 6-inch square central obstruction. After a set of test runs were made and analyzed, the central obstruction was increased to an 8-inch square, which is shown being placed into the filter slot in Fig. 5. The larger obstruction was used for all prototype test results given in this report.

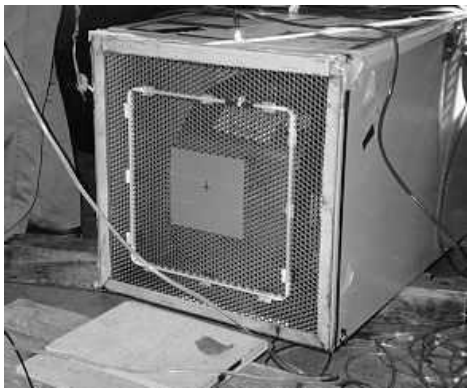

Fig. 4. Prototype installed in filter slot. Return plenum is added to cover prototype.

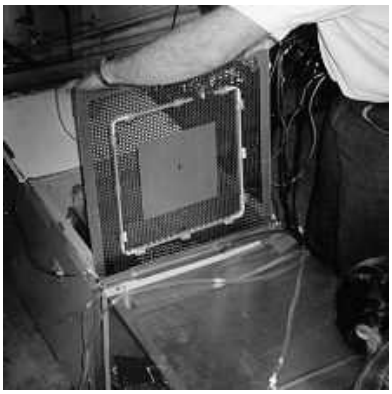

Fig. 5. Prototype with 8-inch masking.

The upstream pressures were measured with a small diameter tube which was centered in the square annular opening where the perforated plate was not masked. There were twelve pressure measurement points which were averaged by the tube. Each measurement point consisted of a small hole facing upstream. This was located in the center of a small "wing" in the form of an upstream facing V-shape which created an upstream total pressure measurement averaged roughly over the projected area of the "wing". This type of sensor arrangement is employed in a number of commercially available flow measurement devices. The downstream pressure measurements employed an identical pressure-averaging tube with twelve simple holes facing downstream, but without the “wings”.

The pressure difference measured with this design was greater than the change in static pressure across the plate. To a first approximation, the upstream pressure was the local static pressure plus one local velocity pressure, where the velocity pressure is $\frac{1}{2}\rho v^2$, ρ is the density of the air, and v is the local air velocity. The downstream pressure was the pressure in the lee of a blunt obstacle. Assuming a pressure coefficient of 0.5, the downstream pressure was the local static minus ½ of the local upstream velocity pressure. Thus the measured pressure difference across the device was approximately the static pressure difference plus 1.5 velocity pressures. The annular opening had an area of about 250 square inches allowing for some obstruction by the tubes and "wings". With a nominal flow of 800 cfm, this gave a velocity of about 460 fpm resulting in a velocity pressure of about 3.3 Pa. The measured pressure difference was therefore about 5 Pa greater than the static pressure difference.

With a typical discharge coefficient of 137 cfm/$Pa^{0.5}$, the measured pressure difference at 800 cfm was about 34 Pa, implying the static pressure difference or pressure loss was about 29 Pa.

This can be compared with pressure losses for a clean 1-inch filter of 10-40 Pa, depending on the type of filter.

At the same time that the prototype was developed, the upstream Duct Blaster® was replaced by another Duct Blaster® manufactured by TEC. This new device was specially calibrated by TEC under the same no-power conditions used in testing to an overall accuracy of plus or minus 1.5 percent. This was used as the "truth" measurement of air flow.

Four standard duct configurations were used to evaluate the effects of inlet geometry and expansion ratio. These four configurations were side entrance with and without the 10-foot duct and top entrance with and without the duct. None of these four configurations used an elbow. A plan view schematic of the side entrance without the duct, as used for the final calibration testing, is shown in Fig. 6 along with schematics of the duct and elbow. Schematics of the top entrance without the duct, the side entrance with the duct, and the top entrance with the duct are shown in the first frame and last two frames of Fig. 7, respectively.

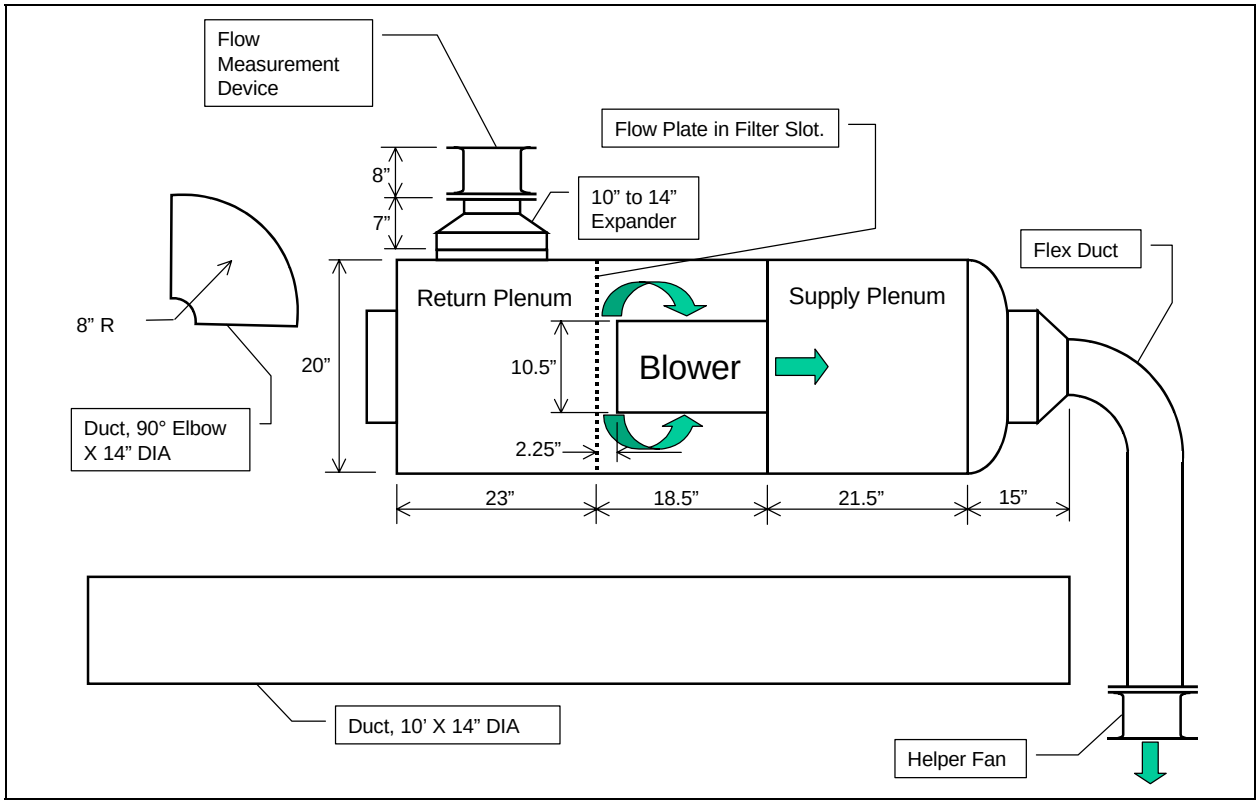

Fig. 6. Schematic of side entrance without duct or elbow configuration, with duct and elbow shown for scaling.

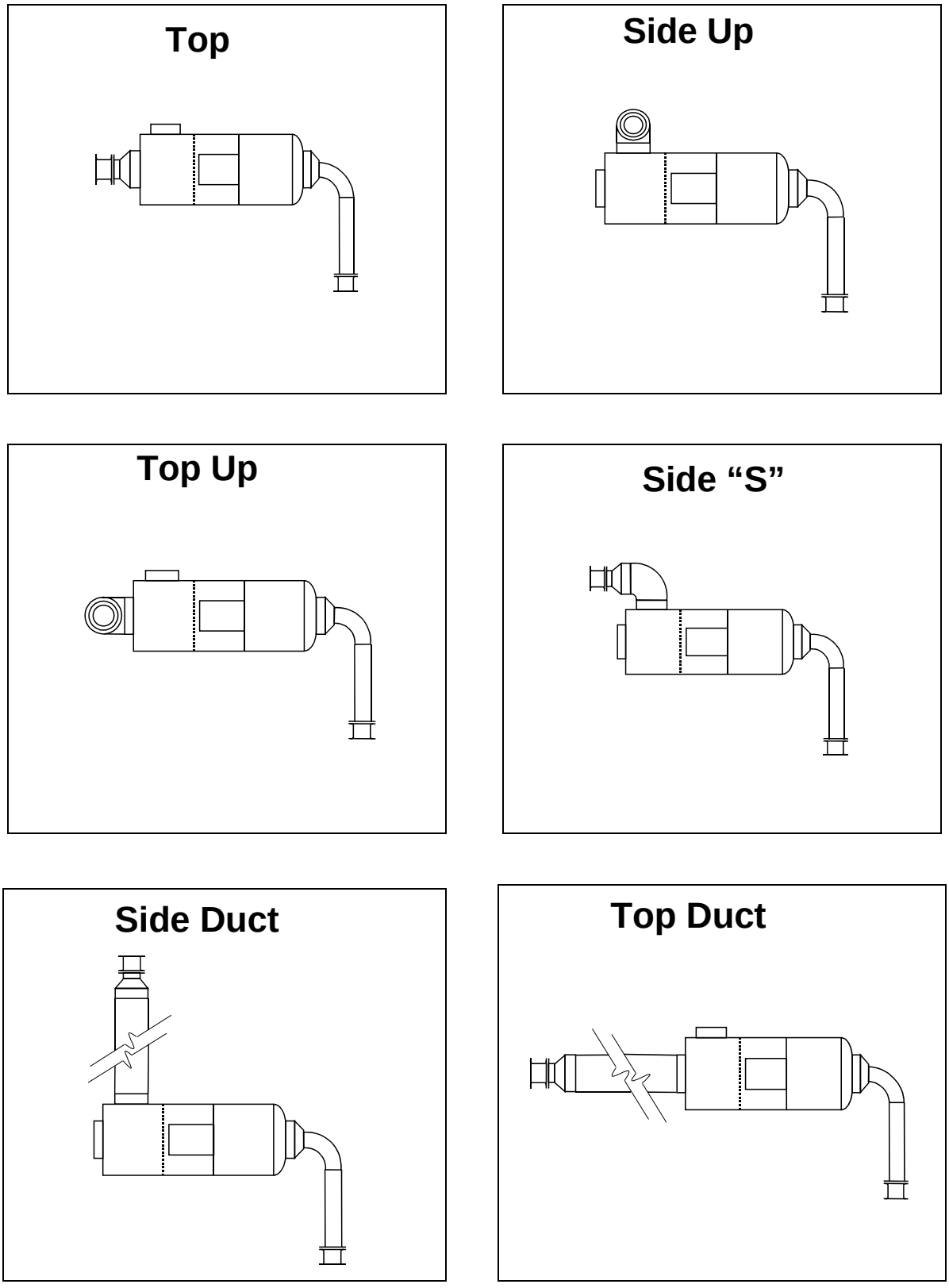

Fig. 7. Return duct configurations used in calibration runs

Three additional configurations involved the use of the round elbow. This was fastened to one of the collars and the expander and measurement device were attached directly to the elbow without the 10-foot duct. The configurations were side with elbow in an "S" configuration, side with the elbow pointing up (i.e. the inlet of the upstream Duct Blaster® faced the ceiling), and top with the elbow pointing up. Plan-view schematics of these three configurations are shown in frames 3 through 5 of Fig. 7. These configurations were used to explore the effects of introducing swirl and altered flow patterns on the accuracy of the measurements.

It should be kept in mind that this is a very difficult flow measurement situation. Consider the side entrance configuration. With no duct there is a jet about 10 inches in diameter entering the return plenum at a right angle to the perforated plate. The centerline of the jet is less than 12 inches upstream of the plate.

Measurement Protocol and Data Reduction

The calibration runs with the final prototype all used the same protocol and data reduction methods. Measurements were made at ten nominal flow stations (no attempt was made to adjust the flows to exact values). The primary emphasis was on flows from 550 cfm to 850 cfm. This range was covered by seven stations at 50 cfm intervals. In addition, measurements were made at 250, 350, and 450 cfm. These were primarily to increase the range for the assessment of the constancy of the discharge coefficients. A more detailed discussion of the results of the measurements at flows below 550 cfm and a comparison of the square root law with using a power law regression fit is given in Appendix A.

It should be noted that different protocols were used and different pressures were measured for some of the early test runs during prototype development. For example, flows below 550 cfm were not included in any of the earlier runs, and because each pressure drop measurement location had to be allocated to a different channel on the data logger, many of the additional pressures were not measured for these early tests.

A 16-channel data logger loaned by TEC was used for all measurements. This device had eight solid state differential pressure transducers and 8 analog channels. The pressure channels had a resolution of 0.1 Pa and a comparable accuracy. Custom software developed by Collin Olson of TEC was used to control the logger. All measurements were recorded as one-second averages. The flow rates were varied by manually setting the flows to a set of predetermined values by adjustment of the downstream helper fan. The software recognized when the flow rate was transitional and marked the points as unstable in the output file. It was also programmed to monitor the standard error of the mean for each of the pressures being measured at each measurements point and to continue taking data until the standard error was below 0.5 Pa. A minimum of 31 one-second values were acquired at each station with additional values if the measurements were very noisy. For the great majority of the measurements, there were 31 one-second values recorded as stable.

For the prototype calibration runs, the measured pressures included the flow pressure from the upstream measurement device, the upstream and downstream pressures from the pressure sensors on the prototype, a static pressure from pitot tube centered in the duct or expander just

upstream from the return plenum, a static pressure at the top of the return plenum, and static pressures upstream and downstream of the perforated plate at one of the corners. In addition, the air temperature just downstream of the upstream flow measurement device was recorded.

For each station, the stable values of the one-second data (usually 31 points) were averaged, resulting in analysis data which were essentially 30-second averages. These values are comparable to what would occur in the field with a single 30-second average measurement using a handheld averaging micro-manometer.

For each flow station a discharge coefficient was calculated from the 30-second data as the flow in cfm measured by the upstream Duct Blaster® divided by the square root of the pressure difference across the perforated plate.

Principal Results

The final prototype was used in an extended series of calibration runs. Each of these runs provided a 30-second discharge coefficient at each of the ten flow stations. Altogether, 43 runs were done using seven different configurations. The four primary calibrations were side and top entrance without the duct and side and top entrance with the duct. In addition, there were three configurations using a 14-inch round elbow attached to one of the collars with the upstream Duct Blaster® attached directly to the elbow via the expander. The first of the configurations with an elbow used the side entrance with the elbow facing toward the top (resulting in an "S" shaped flow path). The second configuration used the side entrance with the elbow facing up toward the ceiling, and the third used the top entrance with the elbow facing up. Because the flow geometry is nearly symmetric with the top entrance, the results for other directions of the elbow would presumably have been very similar. These configurations are shown in the drawings in Figs. 6 and 7, above.

The primary results of this study are given in Table 2. The values in the table are based on seven flow stations ranging from 550 to 850 cfm in increments of 50 cfm. The combination of seven flow stations and 43 runs yields a total of 301 individual 30-second discharge coefficients. For each configuration and for the total data set, the table contains the mean value, the standard deviation of the value, the standard deviation as a percentage of the mean value, and the number of data points. This way of calculating the standard deviations answers the question of what the scatter would be across a set of measurements if an individual measured a 30-second discharge coefficient for a flow in the range from 550 to 850 cfm on seven duct systems with these configurations.

As shown in Table 2, the overall mean discharge coefficient was 136.8 cfm/$Pa^{0.5}$ with a standard deviation of 2.3 cfm/$Pa^{0.5}$ which corresponds to 1.7% of the mean value. The maximum and minimum of the 301 individual values were 143.5 and 132.0 respectively. Thus all 301 values fell within a range of plus or minus 4.3% of the mean value. The performance of the final prototype was excellent.

Table 2. Seven-point calibration results for seven duct configurations

Duct Configuration	C_d (cfm/Pa$^{0.5}$)	Std. Deviation (cfm/Pa$^{0.5}$)	Difference from Overall, %	Number of points
Side with no duct or elbow	138.3	2.4	1.1	49
Top with no duct or elbow	138.8	1.5	1.5	49
Side with 10’ duct, no elbow	136.0	1.8	-0.7	49
Top with 10’ duct, no elbow	135.5	1.5	-1.0	49
Side with no duct, elbow in “S”	136.7	2.3	-0.1	35
Side with no duct, elbow up	135.4	2.1	-1.0	35
Top with no duct, elbow up	136.1	1.7	-0.5	35
Overall	136.8	2.3		301

The individual rows give the results for each of the seven configurations. The top and side entrance with no duct gives discharge coefficients about two percent higher than the others due to the narrower, higher velocity jet. The standard deviations for the individual configurations are on average a bit smaller than for the total as one would expect if there were real differences between the discharge coefficients for the different configurations.

It should be noted that the scatter in the discharge coefficients reflects not only any systematic variations due to the different configurations and slight departures from an exact square-root relationship between pressure and flow, but also the random noise in the 30-second measurements, random variations in the degree of sealing of the return system, variations in absolute atmospheric pressure, and variations in indoor temperature.

These results are presented graphically in Figs. 8, 9, and 10, which show boxplots for each of the configurations and for the total sample. The middle line in the boxplots is the median value, the upper and lower boundaries are the quartiles, the "whiskers" are at roughly the 99th percentile, and the isolated circles are outliers. In each graph, the average discharge coefficient is shown by a horizontal line at 137 cfm/Pa$^{0.5}$. Also in each graph there is a box-plot at the right edge labeled Total, which summarizes all 301 discharge coefficients.

Figure 8 is scaled to the range of the data to emphasize the small differences between configurations. The tendency for the side and top entrance with no duct or elbow to be somewhat higher is clear, as these boxes show less overlap with the others. Figure 9 shows the data with zero on the scale so the eye perceives the percentage variation of the data. On this scale, the discharge coefficients are very similar.

Fig. 10 shows the variation of the discharge coefficients with flow station. It is auto-scaled in order to show clearly the small variations in discharge coefficient. There is a slight upward trend with larger flow rates. The distribution of discharge coefficients for each flow station is asymmetric; the quartile boxes are elongated above the median and the upper whiskers are longer than the lower ones. This is mostly due to the runs without ducts which had higher discharge coefficients than the others. This also results in the median being somewhat lower than the mean value, both within stations and for the sample as a whole.

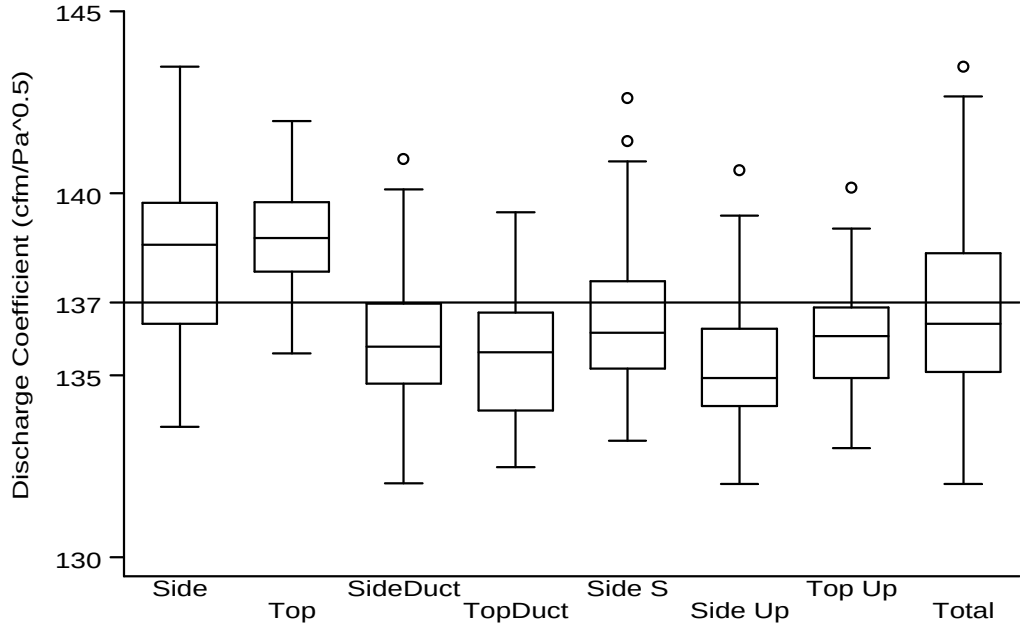

Fig. 8. Discharge coefficients by return type.

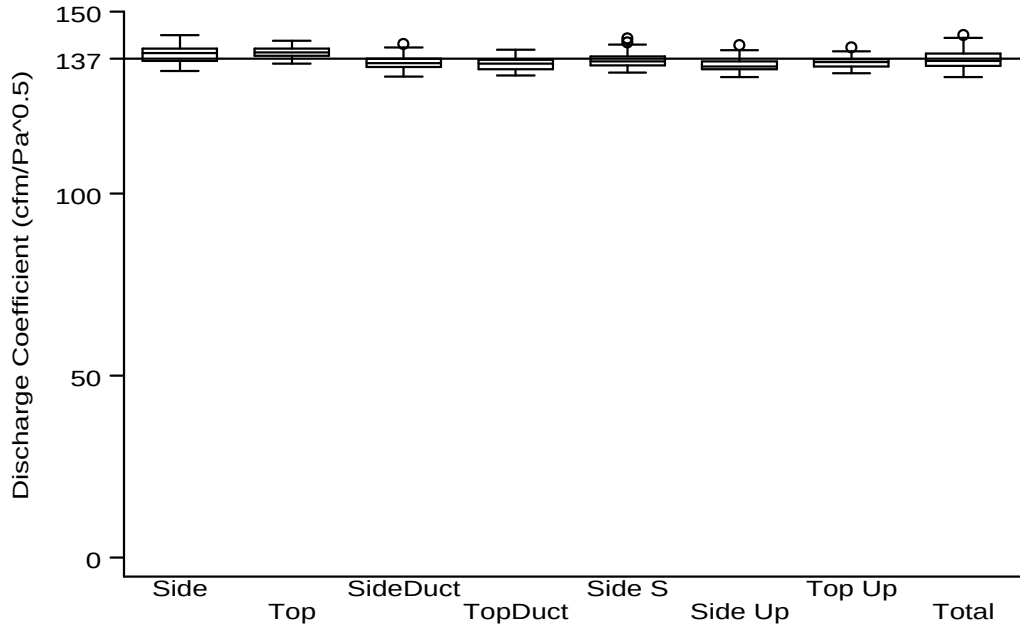

Fig. 9. Discharge coefficients by return type (scaled with zero).

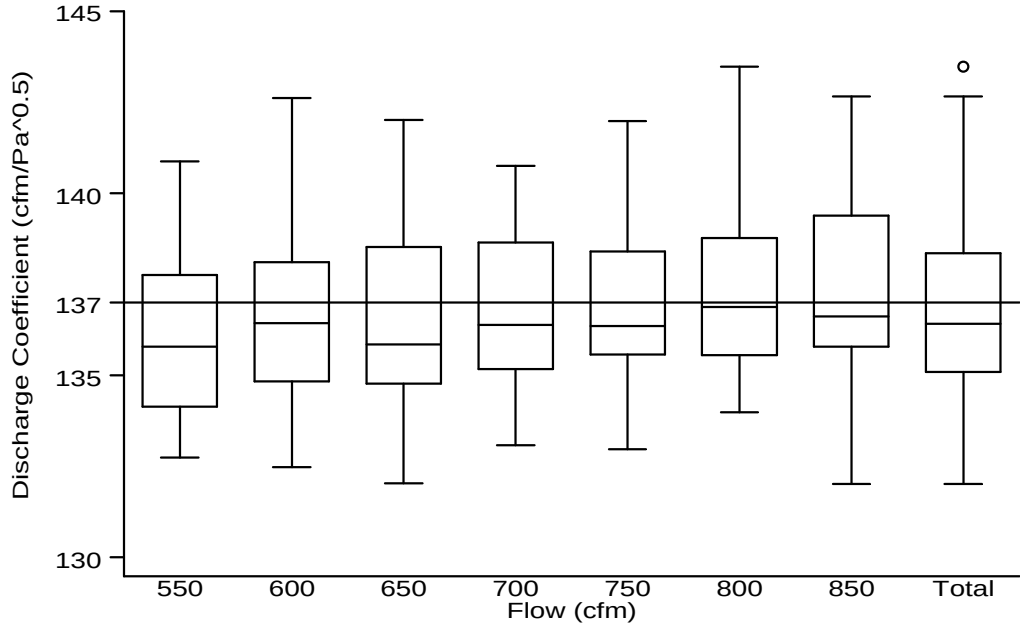

Fig. 10. Discharge coefficients by flow station.

One additional concern that was raised by several members of the project team was whether the close proximity of the air handler blower to the perforated plate had a substantial impact on the measurements. To address this concern, a series of tests were done with an additional 20 inches between the perforated plate and the blower. This resulted in a decrease of the discharge coefficient of about 2.2 percent. See Appendix B for more details.

Further Work

This study is only a proof-of-concept evaluation. While the results are promising, substantial additional work will be required to develop and market a viable commercial product. We briefly list some important issues which must be addressed.

There are several air handler configurations in common use which are sufficiently different from the test configurations to require separate investigation. One such configuration is the typical Western US manufactured home in which a down-flow air handler is mounted in a louvered closet. There is no return plenum or duct. The air enters the filter in an essentially free-air fashion, although it may turn out that closet size, louver size, and louver location may be important factors.

A second common configuration is a standard up-flow gas furnace in which a long narrow filter is located in the side of the return plenum at the bottom of the unit. The latter configuration requires a more elongated perforated plate.

An additional problem is presented by the typical down-flow gas furnace which, in our experience, lacks a filter slot. Instead, the duct installer fits a support bar in the return plenum,

against which two filters are leaned in an A-frame or teepee configuration. It is often difficult to remove or replace the filters in these installations, and often significant flow bypasses the filters.

Another practical problem is the fact that there are about 40 different filter sizes for residential air handlers, although the majority of installations involve only a few of the most common sizes. A strategy must be developed to deal with this issue. One possibility is to make perforated sensing elements in a few sizes with some sort of adjustable masking frame. For example, a 16-inch square plate could be used for 16x16, 16x20, 20x20, and 22x20 inch filter slots. Further testing and calibration will be required to determine the feasibility of this approach.

More work is required to refine the prototype so that a low-cost, easily-calibrated, robust device can be easily manufactured. This will also require further testing and calibration.

Finally, the prototype devices should be field tested on a suitable sample of homes which have a variety of air handler configurations. The results from the prototypes would be compared with results from using a Duct Blaster® to measure the flow and the industry standard temperature difference method for flow measurement.

Summary

A prototype device, suitable for easy field measurement of air handler flow, was developed and evaluated over a variety of flow rates and return plenum configurations. The final calibrations of the finished prototype were done on seven different return plenum configurations. With repetitions, this resulted in 43 separate test runs. In each test run, the device was calibrated at seven different flows, yielding a total of 301 individual calibrations. Each calibration was based on a 30-second average measurement of the pressure difference across the plate and the flow through a specially calibrated Duct Blaster® used as the "truth" measurement.

The mean discharge coefficient of the 301 calibrations was 136.8 cfm/$Pa^{0.5}$ with a standard deviation of 2.3 cfm/$Pa^{0.5}$ which is 1.7% of the flow. The maximum and minimum of the 301 discharge coefficients fell within 4.3% of the mean value.

Considering the intrinsic difficulty of the flow measurement situation, these results should be considered excellent and provide a convincing proof of the concept. The final results showed a great improvement over the initial results with corner taps upstream and downstream of a simple perforated plate. Most of the improvement was due to the development of more sophisticated methods of conditioning the flow by use of a central obstruction, and an increase in the number of pressure measurement points.

Although the results show considerable promise, additional development work will be required to refine the design and address a number of practical problems before a successful commercial product is completed.

Appendix A – Comparison of square root vs. power law relationship between pressure drop and flow rate

One issue that was addressed in this project was whether a square root relationship between air flow rate and pressure drop was sufficient for calibration of the plate or whether a more generalized power law relationship was required. Because it would simplify the calibration of the plate and the resulting equation it is preferable to use a square root law if possible.

The relationship between the pressure drop across the plate and the flow rate can be expressed as

$$Q = K\Delta P^n$$

where Q is the flow rate
K is the flow coefficient
ΔP is the pressure drop across the plate
n is the flow exponent

For flow through an orifice, the exponent should be about 0.5. However, the apparent exponent can deviate from this due to issues such as Reynolds number effects. For each calibration run, the logarithm of the pressure drop across the plate was regressed on the logarithm of the flow measured by the upstream Duct Blaster. This provides the exponent and the logarithm of the flow coefficient. See Appendix C for a table detailing the discharge coefficient C_d (defined as the flow coefficient K in the special case where the exponent is 0.5) and the flow coefficient and exponent for each run. To obtain a flow coefficient and exponent for each return duct configuration aggregated over all tests, the 31-second averages of nominal flow and pressure drop from each test were averaged and the regression of the associated logarithms was done as described above.

We evaluated the adequacy of the square root law in several different ways. One way was to compare the discharge coefficient with the flow coefficient and an exponent of 0.5 with an estimated flow coefficient for each return duct configuration. To do this, all of the data for each flow station in each duct configuration were aggregated. For the square root law, the nominal flow for each flow station from 550-850 cfm was divided by the square root of the corresponding average pressure drop to get the discharge coefficient. For the more general power law, the logarithm of the average pressure drop at each flow was regressed on the logarithm of the nominal flow. This provided the flow exponent n and the logarithm of the flow coefficient K. Since the range of flows from 550-850 cfm is small, the process for obtaining the general power law was repeated with the flows from 250-450 cfm added to the regression. Table A1 shows the resulting discharge coefficients C_d, flow coefficients K_7 and K_{10}, and flow exponents n_7 and n_{10} for each return duct configuration. The subscripts "7" and "10" refer to the number of flow stations considered.

This table shows that, with the exception of the side entrance with no duct or elbow, all of the exponents are quite close to 0.5, and that the exponent for the side with no duct or elbow gets

closer to 0.5 with the additional flow stations. These results suggest that the general power law is not very different from the square root relationship. It is worth noting that, for the majority

Table A1. Comparison of square root and power law calibration curves

	C_d (n=0.5)	K_7	n_7	K_{10}	n_{10}
Side with no duct or elbow	138.3	130.5	0.518	132.7	0.513
Top with no duct or elbow	138.8	138.1	0.502	137.7	0.503
Side with 10’ duct, no elbow	136.0	132.8	0.507	133.0	0.506
Top with 10’ duct, no elbow	135.5	134.1	0.503	135.1	0.501
Side with no duct, elbow in "S"	136.7	137.7	0.498	136.2	0.501
Side with no duct, elbow up	135.4	134.0	0.503	132.4	0.507
Top with no duct, elbow up	136.1	135.7	0.501	135.4	0.501

of individual runs, the exponent was closer to 0.5 when the larger range of flows was used. In addition, the 95% confidence interval on the exponents included 0.5 for the majority of runs. Both of these trends lend additional weight to the notion that the general power law does not deviate significantly from the square root relationship.

Another way to investigate the difference between the square root relationship and a general power law is to plot the discharge coefficients for each flow station vs. the flow station for a return duct configuration. A marked slope indicates that the exponent is truly different from 0.5.

Figure A1 shows two such curves, one for the side without the duct or elbow and one for the top without the duct or elbow. This shows that there is a noticeable slope for the side entrance case, which had the exponent that deviated from 0.5 the most, while there is no distinct slope noticeable for the top entrance. Figure A2 shows the same data with the y-axis rescaled to include zero. This shows that the percentage difference between the two curves is small, and approaches zero at the higher flows where the air handler normally operates. Therefore, while the square root law may not be entirely accurate for all duct configurations, the error in using it is small.

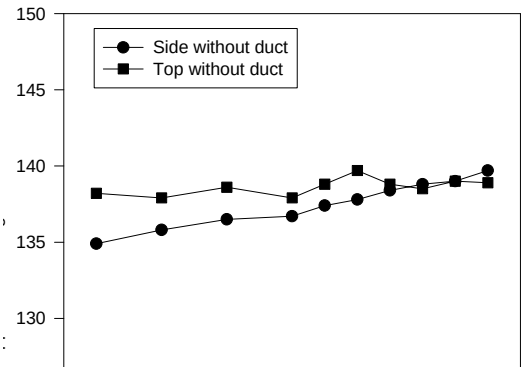

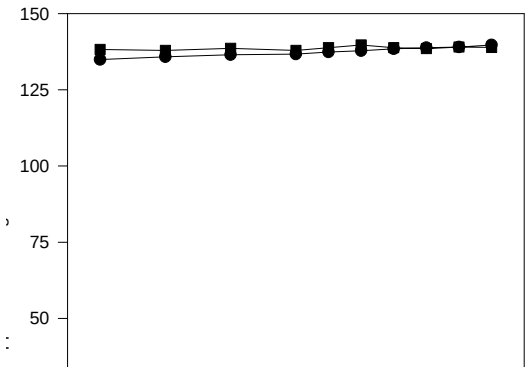

Figure A1. Discharge coefficient vs. air flow rate for side and top without duct.

Figure A2. Discharge coefficient vs. air flow rate for side and top without duct, rescaled with zero.

A third way to investigate the square root vs. power law situation is to investigate how well the two fits based only on the higher flows (550-850 cfm) extrapolate to the lower flows of 250-450 cfm. Figures A3 and A4 show two examples of this type of comparison. In these figures, it is the differences between estimated and measured flow that are plotted against the measured flow. Figure A3 shows a case where the exponent was significantly smaller than 0.5 (n=0.479), and Fig. A4 shows a case where the exponent was significantly above 0.5 (n=0.520). Both figures show that the power law is further from measured flows below 550 cfm than is the square root law, suggesting that a square root calibration would be preferable.

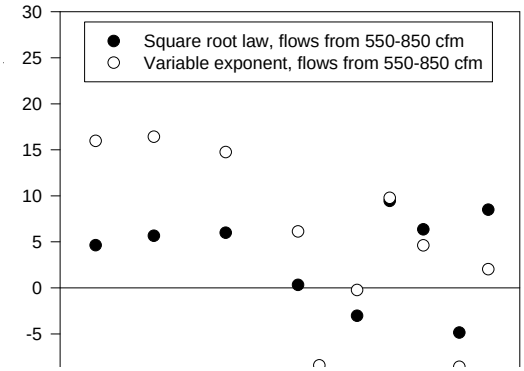

Figure A3. Comparison of seven-point square root and power law extrapolation to low flows for a case where the exponent is significantly below 0.5.

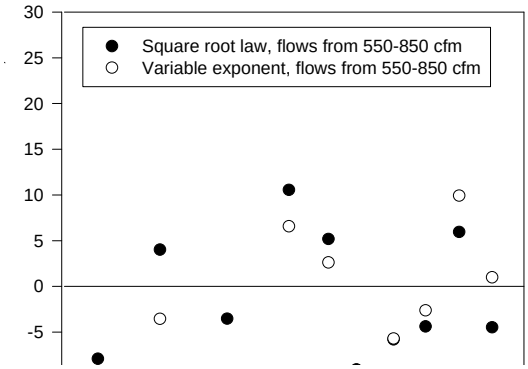

Figure A4. Comparison of seven-point square root and power law extrapolation to low flows for a case where the exponent is significantly above 0.5.

All of the preceding lines of analysis suggest that the square root characterization of the perforated plate calibration is sufficient. Since this is also much simpler and does not change from test to test, the square root was selected as the best method of calibration.

Appendix B – Investigation of the effect of the proximity of the air handler fan to the plate on discharge coefficient

One concern that was raised by several members of the design team was the possibility that the air handler fan, which was only 2.25 inches away from the perforated plate, was having a large impact on the measured discharge coefficient due to this proximity. To address this problem, an additional 20-inch high, 20x20 inch square extension was placed between the return plenum and air handler cabinet. The prototype was attached at the plenum end of this extension, such that the distance between the prototype and the air handler fan was increased to 22.25 inches.

Calibration runs were done for each of the four standard configurations without the round elbow, as well as for the configuration in which the elbow was used to make an "S" shape flow path. The resulting discharge coefficients are presented in the first column of Table B1. The second column shows the average discharge coefficient for the tests of each of the configurations without the extension, and the third column gives the percentage difference, using the results without using the extension as a reference.

Table B1. Discharge coefficients with and without the 20-inch extension

Duct configuration	C_d with 20-inch extension	C_d without extension	Percent difference
Side with no duct or elbow	136.0	138.3	-1.7
Top with no duct or elbow	136.6	138.8	-1.6
Side with 10' duct, no elbow	132.2	136.0	-2.8
Top with 10' duct, no elbow	131.5	135.5	-3.0
Side with no duct, elbow in "S"	134.0	136.7	-2.0

This table shows that the largest discrepancy is 3 percent, with an average over these five duct configurations of about 2.2 percent. In all cases the use of the extension reduces the discharge coefficient. However, this discrepancy is not considered to be a problem, as the results are still within the desired precision of the device.

Appendix C – Detailed results

Table C1 shows the results of each run for each of the standard four configurations (i.e. no elbow used). The subscripts "10" and "7" indicate how many of the ten flow stations were used in the calculation. When only seven flow stations were used, those flows were 500-850 cfm. C_d is the generalized discharge coefficient assuming a flow exponent of 0.5, K is the generalized flow coefficient assuming a power law fit with variable exponent, and n is the power law exponent.

Table C1. Detailed calibration results for four standard duct configurations

Case	Date	$C_{d,10}$	$C_{d,7}$	K_{10}	K_7	n_{10}	n_7
Side no duct	1/30	141.7	141.6	141.7	135.1	.500	.515
	2/03	138.5	139.8	128.0	126.5	.528	.531
	2/03	136.4	137.8	127.3	125.1	.525	.530
	2/13	134.4	135.5	127.1	127.0	.519	.520
	2/13	135.3	135.6	133.0	124.8	.506	.526
	2/18	138.4	139.0	133.5	133.1	.513	.513
	2/18	137.8	138.5	134.3	124.7	.509	.533
	Avg.	137.5	138.3	132.1	128.0	.514	.524
Top no duct	1/30	141.4	140.7	145.6	140.7	.489	.500
	2/03	138.3	139.1	134.1	139.2	.511	.500
	2/03	139.1	139.4	138.1	143.4	.503	.491
	2/13	137.2	138.4	129.1	129.6	.521	.520
	2/13	139.6	139.5	139.6	137.0	.500	.506
	2/18	137.4	137.4	136.6	133.1	.502	.510
	2/18	137.6	137.3	138.9	137.9	.497	.499
	Avg.	138.7	138.8	137.4	137.3	.503	.504
Side duct	1/30	137.1	137.7	134.5	147.6	.507	.479
	1/30	136.9	137.4	135.7	141.5	.503	.491
	2/03	135.0	135.2	134.2	133.4	.502	.504
	2/18	135.6	135.6	136.5	127.3	.498	.520
	2/18	134.2	134.6	131.6	122.3	.507	.529
	2/26	134.9	135.4	132.1	130.9	.507	.510
	3/06	134.6	135.7	125.7	120.4	.524	.537
	Avg.	135.5	136.0	132.9	131.9	.507	.510
Top duct	1/30	137.1	137.3	135.6	131.9	.504	.512
	2/03	133.9	133.6	135.2	129.9	.497	.509
	2/03	134.1	134.4	132.5	133.9	.504	.501
	2/18	137.3	136.6	143.1	139.6	.485	.493
	2/18	135.9	136.0	134.9	131.4	.503	.511
	2/26	134.6	134.8	134.8	136.4	.499	.496
	3/06	134.5	135.5	127.9	129.1	.518	.515
	Avg.	135.3	135.5	134.9	133.2	.501	.505
Avg. of above 4 Avgs.		136.8	137.2	134.3	132.6	.506	.511

Table C2 shows the results for each of the three configurations in which the elbow was used. At the end of Table C2 is a row that shows the average of the averages from all seven duct configurations.

Table C2. Detailed calibration results for three duct configurations with the elbow

Case	Date	$C_{d,10}$	$C_{d,7}$	K_{10}	K_7	n_{10}	n_7
Side "S"	1/30	140.0	140.4	139.1	144.7	.502	.490
	2/13	135.1	135.5	134.4	138.9	.502	.492
	2/13	136.2	135.8	138.7	128.9	.493	.516
	2/26	135.9	136.3	134.6	132.8	.503	.508
	3/06	134.9	135.5	132.4	133.2	.507	.505
	Avg.	136.4	136.7	135.8	135.7	.501	.502
Side up	1/30	138.3	138.8	135.4	129.2	.507	.522
	2/13	133.1	134.2	126.0	135.4	.519	.497
	2/13	134.3	134.8	131.5	130.6	.507	.510
	2/26	135.3	135.5	133.9	131.1	.503	.510
	3/06	133.7	133.9	133.4	133.7	.501	.500
	Avg.	134.9	135.4	132.0	131.9	.507	.508
Top up	1/30	139.1	138.6	142.2	139.7	.492	.498
	2/13	134.7	135.5	129.9	127.3	.513	.519
	2/13	134.7	134.6	136.4	139.8	.496	.489
	2/26	135.8	135.5	137.3	135.4	.496	.500
	3/06	135.4	136.4	129.7	130.2	.515	.514
	Avg.	135.9	136.1	135.1	134.4	.502	.504
Avg. of above 3 Avgs.		135.7	136.1	134.3	133.2	.503	.505
Avg. of all 7 Avgs.		136.3	136.7	134.3	132.8	.505	.508